Breast cancer preoperative 18FDG-PET, overall survival prognostic separation compared with the lymph node ratio

Vinh - Hung, Vincent; Everaert, Hendrik; Gorobets, Olena; Van Parijs, Hilde; Verfaillie, Guy; Vanhoeij, Marian; Storme, Guy; Fontaine, Christel; Lamote, Jan; Perrin, Justine; Farid, Karim; Nguyen, Nam P; Verschraegen, Claire; De Ridder, Mark

Published in:
Breast Cancer

DOI:
10.1007/s12282-021-01234-z

Publication date:
2021

Document Version:
Accepted author manuscript

This is a post-peer-review, pre-copyedit version of an article published in **Breast Cancer**. The final authenticated version is available online at:

https://doi.org/10.1007/s12282-021-01234-z

The Springer Nature SharedIt view-only authenticated version is available at:

https://rdcu.be/cgyyq

Breast cancer preoperative ^{18}FDG-PET, overall survival prognostic separation compared with the lymph node ratio

Vincent Vinh-Hung[1,2]; Hendrik Everaert[1]; Olena Gorobets[2]; Hilde van Parijs[1]; Guy Verfaillie[1]; Marian Vanhoeij[1]; Guy Storme[1]; Christel Fontaine[1]; Jan Lamote[1]; Justine Perrin[2]; Karim Farid[2]; Nam P. Nguyen[3]; Claire Verschraegen[4]; Mark De Ridder[1]

[1] Universitair Ziekenhuis Brussel, 1090 Brussels, Belgium.

[2] University Hospital of Martinique, 97200 Fort-de-France, Martinique, France.

[3] Howard University, Washington, DC 20060, USA.

[4] Ohio State University Comprehensive Cancer Center, Columbus, OH 43210, USA.

Correspondence: Vincent Vinh-Hung, MD, PhD, Oncologisch Centrum, UZ Brussel, Laarbeeklaan 101, 1090 Jette, Belgium. Tel +32 2 477 6040; +33 652 411 567. email: vh@onco.be . ORCID 0000-0002-6403-6120.

Abstract

Purpose:

To evaluate the overall survival prognostic value of preoperative 18F-fluorodeoxyglucose positron emission tomography (PET) in breast cancer, as compared with the lymph node ratio (LNR).

Methods:

Data was abstracted at a median follow-up 14.7 years from a retrospective cohort of 104 patients who underwent PET imaging before curative surgery. PET-Axillary|Sternal was classified as PET-positive if hypermetabolism was visualized in ipsilateral nodal axillary and/or sternal region, else as PET-negative. The differences of 15 years restricted mean survival time ΔRMST according to PET and LNR were computed from Kaplan-Meier overall survival. The effect of PET and other patients' characteristics was analyzed through rankit normalization, which provides with Cox regression the Royston-Sauerbrei *D* measure of separation to compare the characteristics (0 indicating no prognostic value). Multivariate analysis of the normalized characteristics used stepwise selection with the Akaike information criterion.

Results:

In Kaplan-Meier analyses, LNR >0.20 versus ≤0.20 showed ΔRMST=3.4 years, P=0.003. PET-Axillary|Sternal positivity versus PET-negative showed a ΔRMST=2.6 years, P=0.008. In Cox univariate analyses, LNR appeared as

topmost prognostic separator, D=1.50, P<0.001. PET ranked below but was also highly significant, D=1.02, P=0.009. In multivariate analyses, LNR and PET-Axillary|Sternal were colinear and mutually exclusive. PET-Axillary|Sternal improved as prognosticator in a model excluding lymph nodes, yielding a normalized-hazard ratio of 2.44, P=0.062.

Conclusion:

Pathological lymph node assessment remains the gold standard of prognosis. However, PET appears as a valuable surrogate in univariate analysis at 15 years follow-up. There was a trend towards significance in multivariate analysis that warrants further investigation.

Keywords

Positron Emission Tomography; ^{18}F-fluorodeoxyglucose; Predictive factor; D-measure of prognostic separation; normalized hazard ratio; Prognostic ranking method; Lymph node ratio.

Introduction

^{18}F-fluorodeoxyglucose (^{18}FDG) is a radiopharmaceutical positron emitter glucose analog that is taken up by cells through the glucose transport and metabolism [1]. Tissues with increased glycolytic activity can be detected and displayed by three-dimensional image reconstructed through positron emission tomography (PET). In breast cancer, high metabolism shown by ^{18}FDG-PET relates with unfavorable surgical-pathological characteristics [2, 3]. Meta-analyses evidenced that preoperative ^{18}FDG-PET detected occult distant metastases in early breast cancer and could predict higher risks of recurrence or progression [4]. However, the value of ^{18}FDG-PET with respect to prediction of overall survival has been contradictory, possibly due to short follow-up [5, 6]. Out of 15 studies with 3574 patients [5], and 20 studies with 3115 patients [6], the pooled average follow-up were 48.7 and 39.6 months, respectively. Likewise, our previous study of preoperative PET found regional nodal hypermetabolism was significantly associated with a poorer disease-free survival but failed to show a difference in overall survival with a follow-up of 59 months [3].

Demonstrating a long-term impact on overall survival is critical if the role of preoperative ^{18}FDG-PET is to be firmly established. The present study primary objective is to re-assess patterns of ^{18}FDG-PET before surgery as predictors of long-term overall survival. The second objective is to compare ^{18}FDG-PET with other prognostic markers, with special focus on the lymph

node ratio. A third objective is to evaluate the value of ^{18}FDG-PET in very early breast cancer presenting with stage T1 (tumor size ≤ 20 mm).

Patients and Methods

Context

This single center study was approved by the Ethics Committee of the Universitair Ziekenhuis Brussel (UZ Brussel; registration ISRCTN17962845). The protocol was designed to be compliant with the Reporting Recommendations for Tumor Marker Prognostic Studies (REMARK) . Patients treated in 2002-2008 were previously identified, representing a population cohort of 104 cases [3]. The patients selected had histologically confirmed non-metastatic primary breast cancer and had ^{18}FDG-PET performed prior to surgery. Exclusion criteria were previous history of cancer, primary sarcoma of the breast, noninvasive carcinoma, palliative surgery for symptom control, and metastatic disease demonstrated by imaging modes other than ^{18}FDG-PET.

Data

Data collected for the study were age at diagnosis, sex, histological tumor type, pathological grade, hormone receptor status, Her2/neu status, lymphovascular invasion, tumor laterality, tumor location, stage, pathological tumor size, stage, number of examined axillary lymph nodes (*nex*), number of involved axillary lymph nodes (*npos*), neoadjuvant therapy, type of surgery, adjuvant chemotherapy, adjuvant hormone therapy, and adjuvant radiation therapy. Bilateral breast cancer retained only the side with more advanced tumor. The lymph node ratio was computed as *npos*/*nex*, and the log odds

positive nodes, aka empirical logistic transform, as Log_e [(*npos*+0.5)/(*nex*–*npos*+0.5)] [7]. Dichotomized lymph node ratio used a cut-point of 0.20 [8].

PET

Whole-body ^{18}FDG-PET images were acquired 60 minutes after 370–536 MBq (average 464 ± 56 MBq) tracer injection using the Siemens ECAT Accel PET scanner [9]. PET reports were visually assessed for the presence or absence of increased metabolism in different regions of interest: ipsilateral breast (PET-Breast), ipsilateral axillary and/or supraclavicular region (PET-Axillary), and sternal-mediastinal region (PET-Sternal). We also considered the Axillary and Sternal regions jointly as a single combined region of interest (PET-Axillary|Sternal). We recorded positivity/negativity in each region as the presence/absence of increased activity in the region, regardless of activity elsewhere.

Restricted mean survival time

Overall survival was analyzed by the time from diagnosis to censoring at last date known alive or to death from any cause. The proportion of survivors over time was estimated using the Kaplan-Meier method [10]. The log-rank test was used to compare the survivals. The expectation of life limited to *n* years, aka restricted mean survival time (RMST) were computed to 15 years using the Irwin method [11]. The RMST equates the area under a survival curve [12]. The difference Δ_{RMST} between two survival curves is the area between the curves, providing a Kaplan-Meier based measure of separation

that indicates how widely the curves differ. The two-sided z-test was used to compare the RMST's.

Rankit transform, normalized hazard ratio, D measure

Next to the Δ_{RMST}, we considered the Royston-Sauerbrei *D* measure of prognostic separation. The variables representing the measurements of patient's characteristics were transformed into expected values of the standard normal order statistics (rankits), which were then scaled by kappa, where kappa=sqrt(8/PI) ≃ 1.60 [13]. Rankit substitution converts data into its equivalent standard normal distribution. The mean of a half-normal standard distribution is sqrt(2/PI) = sqrt(8/PI)/2 = kappa/2. Dividing the rankits by kappa ascertains that the mean of the scaled half normal values is 0.5 for positive rankits, and –0.5 for negative rankits. Hence, a regression on the scaled rankits is comparable to a regression on data dichotomized into two equal sized groups. Cox regression applied to the scaled rankits provides the *normalized* hazard ratios (nHR) of the variables. The absolute of the log of the normalized hazard ratio is Royston-Sauerbrei's *D* measure of prognostic separation [13]. Test of *D* null (no prognostic value) is based on its standard error derived from the Cox regression.

Multivariate selection

The joint effect of variables transformed into scaled rankits was analyzed in multivariate Cox regression models. Stepwise regression used the Akaike Information Criterion (AIC) to select variables. The AIC is computed as

twice the model's number of parameters, minus twice the model's log likelihood [14]. A variable is considered informative and is included if the penalty of adding a parameter is offset by a sufficient increase of log likelihood. We ran alternative AIC stepwise regressions that included or excluded pathology lymph node data. Bootstrap resampling was applied to verify the stability of models [15].

Software

All analyses used R version 3.6.3 [16]. Missing variables in over 20% of the records were excluded (Supplementary Figure SF1). Multiple imputation by chained equations was used for the remaining missing variables [17]. PET data were not imputed. The software packages used were *survival* (logrank, Kaplan-Meier, Cox regression) [18], *survRM2* (restricted mean survival time) , *survminer* (survival curves) with *ggplot2* (general plotting) , *bootStepAIC* with *MASS* (stepwise AIC) [15], and *mice* (multiple imputation) [17]. Variables transform into rankits used an in-house function, *rnktt*, shared with the study data, reproduced in Supplementary Material, Appendix A.

Results

Patient characteristics

At the cutoff date of January 31, 2020, the median follow-up of the 104 patients was 14.7 years, range 0–16.9. The patient characteristics are summarized in Table 1. Median age of the patients was 58 years, range 33–83. Bilateral breast cancer was diagnosed in 5 (4.8%) patients. Histology was predominantly invasive ductal in 84 (80.8%) patients, Neu score was 2+ versus 0-1 or unknown in 47 (45.6%). Primary systemic therapy was given to 19 (18.3%) patients, radiotherapy to 96 (92.3%), adjuvant hormone therapy to 88 (84.6%). These characteristics did not differ between the two patient groups classified by tumor size ≤ 20mm vs > 20 mm. Other clinical characteristics that differed significantly, as listed in Table 1, reflect expected associations with tumor size, including advanced stage, lymph node involvement, receptor status, grade, lympho-vascular invasion, mastectomy, nodal examination. Likewise, PET positivity was more frequent in patients with tumors > 20 mm (Table 2).

Overall survival

A total of 28 (26.9%) patients died (Supplementary Table ST1); death was associated with metastatic disease in 22 patients, and disease status was unknown in 6. The estimated 15-years overall survival of the whole patients'

population was 69.7% [95%CI: 60.8–80.0]. The restricted mean survival time at 15 years was 12.4 years [11.5–13.3].

Restricted mean survival time, PET

Patients presenting with PET-Breast positivity had no significantly different mortality as compared with PET-Breast negativity, log-rank P=0.678 (Figure 1, top left panel). Patients presenting with PET-Axillary or PET-Sternal positivity had a significantly increased mortality, P=0.027 and P=0.005, respectively (Figure 1, top right and bottom left panel). The 15-years survival estimates by PET-Axillary positive was 56.9% [42.1–77.0] versus PET-Axillary negative 77.2% [66.9–89.2], and by PET-Sternal positive 33.3% [10.8–100] versus PET-Sternal negative 72.1% [63.1–82.5]. By PET-Axillary|Sternal positivity, the 15-years survival was 54.8% [40.5–74.3], versus 79.6% [69.4–91.3] when PET-Axillary and PET-Sternal were both negative, P=0.006 (Figure 1, bottom right panel).

The 15-years RMST's according to PET-Breast status did not differ significantly between PET-Breast positive and PET-Breast negative patients, Δ_{RMST}=−1.2 years (RMST PET negative – RMST PET positive), P=0.428. The RMST's differed significantly according to PET-Axillary status, 11.1 years among PET-Axillary positive, versus 13.2 years among PET-Axillary negative patients, Δ_{RMST}=2.2 years, P=0.033. The RMST's also differed significantly according to PET-Sternal status and according to combined PET-Axillary|Sternal status: RMST by PET-Sternal positive was 7.6 years versus

negative 12.7 years, Δ_{RMST}=5.1 years, P=0.033, and RMST by PET-Axillary|Sternal positive was 10.9 years versus negative 13.5 years, Δ_{RMST}=2.6 years, P=0.008.

Restricted mean survival time, lymph node ratio

By comparison, a lymph node ratio higher than 0.20 (> 20% positive nodes) was associated with a 15-years RMST of 10.0 years, whereas a lymph node ratio ≤ 0.20 was associated with a RMST of 13.4 years, Δ_{RMST}=3.4 years, P=0.003. This corresponds to a separation according to the lymph node ratio wider than the separation according to PET-Axillary|Sternal status. However, the Δ_{RMST} by lymph node ratio and the Δ_{RMST} by PET-Axillary|Sternal did not differ significantly, P=0.598. Figure 2 overlays the lymph node ratio survival curves with the PET-Axillary|Sternal survival curves previously computed (Figure 1, bottom right). In keeping with the non-significant difference in Δ_{RMST}, Figure 2's pairwise comparisons show that low-risk lymph node ratio had survival comparable with negative PET-Axillary|Sternal, and high-risk lymph node ratio had survival comparable with positive PET.

Subgroup analysis by tumor size

By subgroup analysis among patients with tumor size >20 mm, the PET mortality separation was wide with Δ_{RMST}=3.0 years, P=0.015, comparable to the lymph node ratio Δ_{RMST}=3.7 years, P=0.012, both concordantly with the logrank P-values (Supplementary Figure SF2, top panels). Among patients with tumor ≤20 mm, the PET separation was narrow and non-significant, Δ_{RMST}=1.6

years and P=0.376, concordantly with the non-significant logrank P=0.390 (Supplementary Figure SF2, bottom left panel). The lymph node ratio separation appeared wider, Δ_{RMST}=4.6 years, however it was not significant P=0.124, in contrast with the significant logrank P=0.034 (Supplementary Figure SF2, bottom right panel).

Normalized hazard ratio and D measure

The univariate Cox analysis of overall mortality is presented in Table 3, with the normalized hazard ratios (column nHR) computed from the rankit transformed variables, and the untransformed hazard ratios (column HR1), computed from untransformed variables. The ordering of Table 3 follows that of Table 1-2. The normalized hazard ratios and the untransformed hazard ratios are comparable, except with the continuous variables for which HR1 is affected by the unit scales used, but not nHR, and with two binary variables, Sex and PET-Sternal, which were associated with highly unbalanced distribution. All pathology indicators of lymph node involvement, notably stage, which is stratified by lymph nodes, were statistically significant. All three PET indicators of regional involvement, PET-Axillary, PET-Sternal, and combined PET-Axillary|Sternal, were also significant and were concordant with the logrank tests (Figure 1).

The *D* measures of prognostic separation were directly obtained from the absolute of the Log of Table 3's normalized hazard ratios. These are presented as forest plot in Figure 3, ordered from top to bottom, from the

largest *D*-measure to the smallest. The variables in the top half included all lymph node indicators (lymph node ratio topmost with $D=\log(4.46)=1.50$, $P<0.001$), the 3 PET regional indicators (of which PET-Axillary|Sternal $D=\log(2.77)=1.02$, $P=0.009$), pathology lymphovascular invasion, sex male, progesterone status, and age, which were all significant.

Multivariate selection

Multivariate analyses were conducted on the normalized variables, excluding Sex because of the imbalance, 2 males vs 102 females, and excluding the PET-Axillary and PET-Sternal status which were combined into a single PET-Axillary|Sternal variable. Consequently, the starting model jointly evaluated 22 variables (Table 4). With 104 patients, that is an uninterpretable bloated model, yielding inconsistencies such as the number of positive nodes "significantly" associated with a reduced risk of death, normalized hazard ratio of 0.09 (Table 4). Pruning is required, which was done by stepwise regression. Out of the 22 variables, 5 were retained by AIC (Table 4, Model A): age, lymph node ratio, primary systemic therapy, adjuvant chemotherapy, and adjuvant hormone therapy, of which the lymph node ratio showed the highest reliability with 95% of bootstrap iterations testing significant, followed by adjuvant hormone therapy, reliability 71%, and age, reliability 60%. The stepwise regression was repeated on the same initial set of covariates but excluding the lymph node pathology variables from start (Table 4, Model B). The regression

also retained 5 variables, of which the most reliable were age (78%), progesterone receptor status (72%), and PET-Axillary|Sternal positivity (52%).

Discussion

Main finding

This study adds to the evidence of an invaluable role of preoperative ^{18}FDG-PET in breast cancer [5, 6]. The most important predictor of mortality in breast cancer is nodal involvement as measured by the lymph node ratio [8, 19]. To our knowledge, this is the first time that a head to head comparison with a marker shows a non-negligible prognostic value as compared with nodal ratios . Regional axillary or sternal PET positivity versus negativity was associated at 15 years with a Δ_{RMST} of 2.6 years, i.e. a difference in prognosis of 2.6/15=17.3%. In comparison, a lymph node ratio of ≤0.20 (low risk) versus >0.20 (intermediate-high risk group) was associated with a Δ_{RMST} of 3.4 years, i.e. a difference in prognosis of 3.4/15=22.7%.

The lymph node ratio was superior to PET by all criteria, by D-measure, by univariate survival, by predicted time-lost, by multivariate stepwise regression, and by tumor size subgroups. The long duration of the lymph node ratio prognosis to 15 years also warrants a special note: it contrasts starkly with biomarkers such as IHC4 or Mammostrat, whose prognostic performances are limited to the first 5 years [20]. However, the lymph node ratio superiority margins compared to PET appears small. Moreover, the prognostic impact of PET is maintained at long term, survival curves continue to separate at over 15 years (Figure 2). Balancing effectiveness for the purpose of prognostication would have to weigh optimal surgical-pathological staging, with the morbidity

of axillary exploration, versus PET which might allow preoperative treatment and dynamic monitoring [21], without the axillary surgical morbidity.

Normalized hazard ratios

Rankits were introduced in 1944 as a statistical tool for the analysis of experiments, much like the probit transforms and normal probability plots [22]. The Royston-Sauerbrei approach provides at once a scaled normalized hazard ratio. Its absolute log, which they called *D*, is a measure of how widely prognostic groups are separated [13]. The 1.60 scaling provides an elegant interpretation of the normalized hazard ratios as variables virtually dichotomized into two equal-size groups, even when the variable is not so. The rankit transform assumes normal distribution, but the authors noted reasonable robustness against departures from normality [13]. The normalized hazard ratios are more easily interpretable than conventional hazard ratios. The normalized hazard ratios adjust for imbalances in binary variables (for example Table 3, Sex male unadjusted hazard ratio 8.28, was normalized 4.10), and are not affected by change of scale in continuous variables (for example Table 3, the lymph node ratio hazard ratio 14.8 applies to a proportion range from 0 to 1, converted to percentage it would have been 1.03=exp(log(14.8)/100) per 1% unit, yet the normalized hazard ratio would remain the same 4.46). The normalized hazard ratio facilitates a clinically meaningful direct comparison of prognostic markers, without affecting

significance test results (Table 3, columns P-nHR and P-HR1, identical values with binary variables, minor differences with continuous variables).

A note on low frequency cases

Male breast cancer is often excluded from clinical trials. Authors have drawn attention to ^{18}FDG-PET in men [3, 23]. Synchronous bilateral breast cancer likewise has often been excluded from preoperative PET studies. Two studies included bilateral cases, 1 of 59 patients,[24], and 5 of 194 patients [25]. Cases were counted twice, providing 60 and 199 breast cancers, respectively. Our patients included 5 bilateral cases, each counted only once to avoid duplicating the survival outcomes. Male breast cancer and bilaterality are of low frequency, we cannot make inferences, but we believe these should be reported to allow data accrual when studies will be pooled.

Models' dependencies; false negatives

There are many dependencies between covariates (Table 1). Lymph node involvement and PET regional nodes positivity strongly correlate (Figure SF3). When two variables match one-on-one, both cannot appear in the same model. Removing the lymph node information from Model A uncovered the PET information in Model B. Interestingly, the literature counterpart of our models' what-if simulations can be found in a study that compared the prognostic utility of preoperative and immediate-postoperative PET [26]. Among 149 patients who underwent ^{18}FDG-PET before neoadjuvant therapy, PET positivity outside the primary tumor was associated with worse overall survival,

P=0.063, and worse disease-free survival, P<0.001. But among 126 patients who underwent ^{18}FDG-PET after surgery and before any adjuvant therapy, no prognostic survival differences. Our study rejoins in the preoperative prognostic utility of ^{18}FDG-PET; postoperatively, the prognostic value is superseded by the lymph node assessments.

Model A and B are likely overfitted, as shown by the bootstrap percentage significance. Each model included 2 variables that were significant in less than half of the iterations; they cannot be used for prediction. Nevertheless, the models can be informative for hypothesis building. We hypothesize that stage, lymph nodes and PET might be considered as expressions of tumor burden. We have previously modeled the effect of the percentage of involved nodes on the mortality in breast cancer as a random walk, arguing that the mortality observed with a given percentage is the result of accumulated effects of preceding nodal involvements [27]. Quantitative PET, not available in this study, could provide a dynamic information in future studies [21, 28].

PET does not detect all sites of disease. In the breast, positivity was observed in 87 of 104 (83.7%) patients; there was no visualizable hypermetabolism in the other 17 (16.3%) patients (Table 2). The false negative rate is concordant with other observations [29]. PET is known to have poor spatial resolution [30]. We did not compare PET with MRI or ultrasound which excel for high precision imaging [31-34]. These modalities can detect

high risk disease [35-37]; there is no doubt on their prognostic value. We believe that medical imaging are not mutually exclusive [28, 29, 34, 38]. Spatial imaging was missing in the present study. We expect further advances in prognostic information with the increased availability of dedicated combined PET/MR equipment [39].

Other limitations

Besides the retrospective nature of the study, affected by recollection bias and a posteriori characterization of patients' data, limitations include the small number of patients, the coarse categorization of PET without blind assessment, using outdated screen printout. Quantitative imaging analysis of PET is likely more efficient than dichotomization, which is subject to error, to lack of precision, to observers' variability, and, inherently, causes loss of information. However, standardized uptake value (SUV) measurements were available in only 36 patients among whom 9 events were observed. The analysis of the SUVs was not retained for the present report, but the data is available in the shared data file.

The study was not designed to evaluate how PET affected the management of the patients. PET-Breast status was not associated with survival. We questioned if that was attributable to confounding by the type of surgery. In an unplanned analysis, we noted that PET-Breast positive patients had a high rate of mastectomy and high rate of adjuvant radiotherapy. Patients who underwent mastectomy represented 72 among 87 (82.8%) PET-

Breast positive patients, versus 6 among 17 (35.3%) PET-Breast negative patients, P=0.0001. However, there was no significant interaction between mastectomy and PET-Breast status on survival, which did not support confounding by the type of surgery. Another potential confounding is the spread of ductal carcinoma in situ which could have affected the breast positivity rate [30, 40]. We did not collect that data. However, we noted one case who presented with invasive carcinoma at initial biopsy. At surgery only in situ carcinoma was found. PET was positive in the breast. At 15 years she is alive without recurrence. That observation raises the question that PET positivity in the breast might not have the same impact as PET positivity in regional areas.

The size of the study was small, able to detect only large effects. The interpretation of results such as the survival curves of Figure 1-2 or the D measures of Figure 3 has to be mitigated by the large overlapping confidence intervals. The multivariate analysis already commented that the cohort of only 104 patients cannot sustain a full analysis of all variables. By the rule of thumbs of 10 events per variable, the data is insufficient to explore relationship between variables. The results indicate the preponderance of prognosis by lymph node ratio over PET or other variables, but uncertainty must be acknowledged.

Strengths

Strengths include the long follow-up; 15 years represent a substantial part of patients' lifeline. Three times more events than previously reported were counted [3], allowing a reasonably powered analysis for up to 3-5 variables. PET-Axillary|Sternal positivity displayed hazard proportionality for overall survival over time, in contrast with disease-free survival that lost proportionality by 10-15 years (Justine Perrin, personal communication). The present results will be the basis for a prospective comparison with a new cohort of patients who have been diagnosed more recently.

This study identifies the importance of metabolic imaging in initial staging, for the patient to avoid non-necessary and potentially health debilitating axillary procedures, yet also not to miss critical information on life expectancy, for the choice of therapy. For survival, the long-term prognostic impact of PET needs to be considered when other markers are evaluated. In clinical studies with the aim of long-term outcome, metabolic information might be required to avoid confounding results in patients with widely differing prognoses.

Conclusion

Pathological lymph node assessment remains the gold standard among prognostic factors. However, along with age and progesterone receptor status, PET is a topmost alternate long-term predictor of breast cancer overall survival. Considering the comparable lifeline prediction, non-invasiveness, and potential for dynamic monitoring, metabolic imaging for therapy decision should be weighed against surgical axillary exploration.

Compliance with Ethical Standards:

Funding:

The study received no funding.

Conflicts of interest:

Vincent Vinh-Hung received non-financial support from AddMedica, AstraZeneca, Bayer HealthCare SAS, Bristol-Myers Squibb, Ipsen Pharma, Janssen-Cilag, GlaxoSmithKline, Pfizer SAS, Roche SAS, Sanofi Aventis France, Sepropharm International.

Vincent Vinh-Hung and Nam P. Nguyen hold a patent on the Mean absolute dose deviation, unrelated to the present study.

Olena Gorobets received non-financial support from AstraZeneca.

The other authors declare that they have no conflict of interest.

Ethical approval:

All procedures performed in the study were in accordance with the ethical standards of the institutional research committee and with the 1964 Helsinki declaration and its later amendments. The study was approved by the Medical Ethics Committee of the Universitair Ziekenhuis Brussel. Informed consent was obtained from all individual participants included in the study.

The study was registered at: http://www.isrctn.com/ISRCTN17962845

Declarations

Data availability:

Data is available on Mendeley.

Temporary link for review:

https://data.mendeley.com/datasets/sfvtmrd8z9/draft?a=f1f1fe69-2387-4d9a-92ca-e564faa046de

Reserved DOI: https://dx.doi.org/10.17632/sfvtmrd8z9.1

Protocol availability:

The protocol is available at:

https://www.protocols.io/view/pet2015uz-prognostic-value-of-pre-treatment-18fdg-bf7jjrkn/abstract

http://www.isrctn.com/ISRCTN17962845

Code availability:

The study used software applications available at:

https://cran.r-project.org/

Function rnktt is available in Appendix A and shared with the data at:

reserved DOI: https://dx.doi.org/10.17632/sfvtmrd8z9.1

Authors' contributions:

VVH and HE designed and conceptualized the study; VVH, HE and MDR drafted the study protocol; VVH and HE analyzed the PET-scan images; VVH, HVP, GV, MV, GS, CF, JL, and MDR contributed patients data; VVH, OG, NPN and CV analyzed the data and wrote the first draft; VVH, OG, HVP, GV, MV, GS, CF, JL, JP, KF, NPN, CV, and MDR revised the manuscript; all authors critically reviewed the manuscript and gave final approval.

References

1. Kurihara H, Shimizu C, Miyakita Y, Yoshida M, Hamada A, Kanayama Y, et al. Molecular imaging using PET for breast cancer. Breast Cancer. 2016; 23: 24-32.

2. Jung NY, Kim SH, Kang BJ, Park SY, Chung MH. The value of primary tumor (18)F-FDG uptake on preoperative PET/CT for predicting intratumoral lymphatic invasion and axillary nodal metastasis. Breast Cancer. 2016; 23: 712-7.

3. Vinh-Hung V, Everaert H, Lamote J, Voordeckers M, van Parijs H, Vanhoeij M, et al. Diagnostic and prognostic correlates of preoperative FDG PET for breast cancer. Eur J Nucl Med Mol Imaging. 2012; 39: 1618-27.

4. Vinh-Hung V, Everaert H, Farid K, Djassemi N, Baudin-Veronique J, Bougas S, et al. Preoperative [18]fluorodeoxyglucose-positron emission tomography/computed tomography in early stage breast cancer: Rates of distant metastases. World J Radiol. 2017; 9: 312-20.

5. Diao W, Tian F, Jia Z. The prognostic value of SUVmax measuring on primary lesion and ALN by (18)F-FDG PET or PET/CT in patients with breast cancer. Eur J Radiol. 2018; 105: 1-7.

6. Wen W, Xuan D, Hu Y, Li X, Liu L, Xu D. Prognostic value of maximum standard uptake value, metabolic tumor volume, and total lesion glycolysis of positron emission tomography/computed tomography in patients with breast cancer: A systematic review and meta-analysis. PLoS One. 2019; 14: e0225959.

7. Vinh-Hung V, Verschraegen C, Promish DI, Cserni G, Van de Steene J, Tai P, et al. Ratios of involved nodes in early breast cancer. Breast Cancer Res. 2004; 6: R680-R8.

8. Liu D, Chen Y, Deng M, Xie G, Wang J, Zhang L, et al. Lymph node ratio and breast cancer prognosis: a meta-analysis. Breast Cancer. 2014; 21: 1-9.

9. Bral S, Vinh-Hung V, Everaert H, De Coninck P, Storme G. The use of molecular imaging to evaluate radiation fields in the adjuvant setting of breast cancer - A feasibility study. Strahlenther Onkol. 2008; 184: 100-4.

10. Kaplan E, Meier P. Nonparametric estimation from incomplete observations. J Am Stat Assoc. 1958; 53 457-81.

11. Irwin JO. The standard error of an estimate of expectation of life, with special reference to expectation of tumourless life in experiments with mice. J Hyg (Lond). 1949; 47: 188.

12. Royston P, Parmar MK. Restricted mean survival time: an alternative to the hazard ratio for the design and analysis of randomized trials with a time-to-event outcome. BMC Med Res Methodol. 2013; 13: 152.

13. Royston P, Sauerbrei W. A new measure of prognostic separation in survival data. Stat Med. 2004; 23: 723-48.

14. Akaike H. A new look at the statistical model identification. IEEE Transactions on Automatic Control. 1974; 19: 716-23.

15. Venables WN, Ripley BD. Modern Applied Statistics with S. Fourth Edition. In: Chambers J, Eddy W, Hardle W, editors. Statistics and Computing. Springer-Verlag: New York; 2002. p. 172-6.

16. R Core Team. R: a language and environment for statistical computing. R Foundation for Statistical Computing. 2020; R version 3.6.3.

17. van Buuren S. Multiple imputation of discrete and continuous data by fully conditional specification. Stat Methods Med Res. 2007; 16: 219-42.

18. Therneau TM, Grambsch PM. Modeling survival data: extending the Cox model (Statistics for biology and health). Springer-Verlag New York, NY 2000. p. 87-152.

19. Liu C, Li H, Zhuo R, Wang L, He L, Ruan Q, et al. Grade-lymph node ratio predicts the survival of breast cancer in different molecular types: A Surveillance, Epidemiology, and End Results population-based analysis. Medicine (Baltimore). 2019; 98: e16436.

20. Stephen J, Murray G, Cameron DA, Thomas J, Kunkler IH, Jack W, et al. Time dependence of biomarkers: non-proportional effects of immunohistochemical panels predicting relapse risk in early breast cancer. Br J Cancer. 2014; 111: 2242-7.

21. Keam B, Im SA, Koh Y, Han SW, Oh DY, Cho N, et al. Predictive value of FDG PET/CT for pathologic axillary node involvement after neoadjuvant chemotherapy. Breast Cancer. 2013; 20: 167-73.

22. Ipsen J, Jerne NK. Graphical Evaluation of the Distribution of Small Experimental Series. Acta Pathol Microbiol Scand. 1944; 21: 343-61.

23. Ulaner GA, Juarez J, Riedl CC, Goldman DA. (18)F-FDG PET/CT for Systemic Staging of Newly Diagnosed Breast Cancer in Men. J Nucl Med. 2019; 60: 472-7.

24. Choi BB, Lee JS, Kim KH. Association between MRI Features and Standardized Uptake Value of 18F-FDG PET/CT in Triple-Negative Breast Cancer. Oncol Res Treat. 2018; 41: 706-11.

25. Higuchi T, Fujimoto Y, Ozawa H, Bun A, Fukui R, Miyagawa Y, et al. Significance of Metabolic Tumor Volume at Baseline and Reduction of Mean Standardized Uptake

Value in (18)F-FDG-PET/CT Imaging for Predicting Pathological Complete Response in Breast Cancers Treated with Preoperative Chemotherapy. Ann Surg Oncol. 2019; 26: 2175-83.

26. Evangelista L, Cervino AR, Michieletto S, Saibene T, Ghiotto C, Guarneri V, et al. Diagnostic and prognostic impact of fluorine-18-fluorodeoxyglucose PET/CT in preoperative and postoperative setting of breast cancer patients. Nucl Med Commun. 2017; 38: 537-45.

27. Vinh-Hung V, Leduc N, Baudin J, Storme G, Nguyen NP, Joachim C, et al. Axillary Lymph Node Involvement in Breast Cancer: A Random Walk Model of Tumor Burden. Cureus. 2019; 11: e6249.

28. Tokes T, Kajary K, Szentmartoni G, Lengyel Z, Gyorke T, Torgyik L, et al. Predictive and prognostic value of FDG-PET/CT imaging and different response evaluation criteria after primary systemic therapy of breast cancer. Breast Cancer. 2017; 24: 137-46.

29. Nakano Y, Noguchi M, Yokoi-Noguchi M, Ohno Y, Morioka E, Kosaka T, et al. The roles of (18)F-FDG-PET/CT and US-guided FNAC in assessment of axillary nodal metastases in breast cancer patients. Breast Cancer. 2017; 24: 121-7.

30. Hayashi M, Murakami K, Oyama T, Domeki Y, Hagiwara S, Katsumata D, et al. PET/CT supports breast cancer diagnosis and treatment. Breast Cancer. 2008; 15: 224-30.

31. Razek AA, Lattif MA, Denewer A, Farouk O, Nada N. Assessment of axillary lymph nodes in patients with breast cancer with diffusion-weighted MR imaging in combination with routine and dynamic contrast MR imaging. Breast Cancer. 2016; 23: 525-32.

32. Kato F, Kudo K, Yamashita H, Baba M, Shimizu A, Oyama-Manabe N, et al. Predicting metastasis in clinically negative axillary lymph nodes with minimum apparent diffusion coefficient value in luminal A-like breast cancer. Breast Cancer. 2019; 26: 628-36.

33. Murakami W, Tozaki M, Nakamura S, Ide Y, Inuzuka M, Hirota Y, et al. The clinical impact of MRI screening for BRCA mutation carriers: the first report in Japan. Breast Cancer. 2019; 26: 552-61.

34. Izumori A, Kokubu Y, Sato K, Gomi N, Morizono H, Sakai T, et al. Usefulness of second-look ultrasonography using anatomical breast structures as indicators for magnetic resonance imaging-detected breast abnormalities. Breast Cancer. 2020; 27: 129-39.

35. Nakashima K, Uematsu T, Takahashi K, Nishimura S, Tadokoro Y, Hayashi T, et al. Does breast cancer growth rate really depend on tumor subtype? Measurement of tumor doubling time using serial ultrasonography between diagnosis and surgery. Breast Cancer. 2019; 26: 206-14.

36. Nagasaka K, Satake H, Ishigaki S, Kawai H, Naganawa S. Histogram analysis of quantitative pharmacokinetic parameters on DCE-MRI: correlations with prognostic factors and molecular subtypes in breast cancer. Breast Cancer. 2019; 26: 113-24.

37. Yuen S, Monzawa S, Yanai S, Matsumoto H, Yata Y, Ichinose Y, et al. The association between MRI findings and breast cancer subtypes: focused on the combination patterns on diffusion-weighted and T2-weighted images. Breast Cancer. 2020; 27: 1029-37.

38. Nguyen-Thu H, Hanaoka H, Nakajima T, Yamaguchi A, Nguyen-Cong T, Kartamihardja AAP, et al. Early prediction of triple negative breast cancer response to cisplatin treatment using diffusion-weighted MRI and (18)F-FDG-PET. Breast Cancer. 2018; 25: 334-42.

39. Tabouret-Viaud C, Botsikas D, Delattre BM, Mainta I, Amzalag G, Rager O, et al. PET/MR in Breast Cancer. Semin Nucl Med. 2015; 45: 304-21.

40. Seo YY, Yoo IR, Park SY, Oh JK, Kim SH, Sohn HS. Ductal carcinoma in situ and ductal carcinoma in situ with microinvasion: correlation of FDG uptake with histological and biological prognostic factors. Breast Cancer. 2017; 24: 353-61.

Tables

Table 1. Patient characteristics by tumor size.

Characteristic	All N = 104	Tumor ≤ 20 mm N = 37	Tumor > 20 mm N = 67 (*)	P-value
Age, years				0.685
Mean (SD)	58.2 (12.5)	58.8 (11.2)	57.8 (13.3)	
Sex				0.055
Male	2 (1.9%)	2 (5.4%)	0 (0.0%)	
Female	102 (98.1%)	35 (94.6%)	67 (100.0%)	
Tumor location				0.632
Central	14 (13.5%)	3 (8.1%)	11 (16.4%)	
Inner quadrants	16 (15.4%)	6 (16.2%)	10 (14.9%)	
Outer quadrants	64 (61.5%)	25 (67.6%)	39 (58.2%)	
Else	10 (9.6%)	3 (8.1%)	7 (10.4%)	
Tumor laterality				0.408
Bilateral	5 (4.8%)	3 (8.1%)	2 (3.0%)	
Left	45 (43.3%)	17 (45.9%)	28 (41.8%)	
Right	54 (51.9%)	17 (45.9%)	37 (55.2%)	
Stage				<0.001
Missing	2	1	1	
I	18 (17.6%)	18 (50.0%)	0 (0.0%)	
IIA	28 (27.5%)	12 (33.3%)	16 (24.2%)	
IIB	18 (17.6%)	0 (0.0%)	18 (27.3%)	
III	34 (33.3%)	4 (11.1%)	30 (45.5%)	
IV	4 (3.9%)	2 (5.6%)	2 (3.0%)	
Pathological tumor size, mm				< 0.001
Mean (SD)	28.2 (16.7)	14.0 (4.9)	36.0 (15.7)	
Number of positive nodes, N				0.103
Missing	5	2	3	
Mean (SD)	3.4 (5.2)	2.2 (5.5)	4.0 (5.0)	
Number of nodes examined, N				0.001
Missing (§)	1 (§)	0 (§)	1 (§)	
Mean (SD)	14.3 (9.1)	10.5 (8.8)	16.5 (8.6)	
Lymph node ratio, fraction				0.046
Missing	5	2	3	
Mean (SD)	0.19 (0.27)	0.12 (0.25)	0.23 (0.27)	
Lymph node ratio dichotomized				0.010
> 0.20	30 (30.3%)	5 (14.3%)	25 (39.1%)	
≤ 0.20	69 (69.7%)	30 (85.7%)	39 (60.9%)	
Log odds positive nodes	0	0	0	0.451
Missing	2	3	5	
Mean (SD)	-1.7 (1.5)	-1.5 (1.5)	-1.6 (1.5)	

Estrogen-progesterone receptors				0.010
Both positive ER+ PR+	67 (64.4%)	30 (81.1%)	37 (55.2%)	
Both negative ER- PR-	20 (19.2%)	6 (16.2%)	14 (20.9%)	
Else	17 (16.3%)	1 (2.7%)	16 (23.9%)	
Neu score				0.437
Missing	1	0	1	
< 2	56 (54.4%)	22 (59.5%)	34 (51.5%)	
≥ 2	47 (45.6%)	15 (40.5%)	32 (48.5%)	
Grade				0.013
Missing	4	1	3	
≤ 2	71 (71.0%)	31 (86.1%)	40 (62.5%)	
> 2	29 (29.0%)	5 (13.9%)	24 (37.5%)	
Lymphovascular invasion				0.008
Missing	20	5	15	
Absent	45 (53.6%)	23 (71.9%)	22 (42.3%)	
Present	39 (46.4%)	9 (28.1%)	30 (57.7%)	
Ductal histology				0.562
No	20 (19.2%)	6 (16.2%)	14 (20.9%)	
Yes	84 (80.8%)	31 (83.8%)	53 (79.1%)	
Primary systemic therapy				0.144
No	85 (81.7%)	33 (89.2%)	52 (77.6%)	
Yes	19 (18.3%)	4 (10.8%)	15 (22.4%)	
Surgery [‡]				0.001
Breast conserving	26 (25.0%)	16 (43.2%)	10 (14.9%)	
Mastectomy	78 (75.0%)	21 (56.8%)	57 (85.1%)	
Radiotherapy				0.862
No	8 (7.7%)	3 (8.1%)	5 (7.5%)	
Postoperative	93 (89.4%)	33 (89.2%)	60 (89.6%)	
Preoperative	2 (1.9%)	1 (2.7%)	1 (1.5%)	
Radiosurgery	1 (1.0%)	0 (0.0%)	1 (1.5%)	
Adjuvant chemotherapy				0.001
No	51 (49.0%)	26 (70.3%)	25 (37.3%)	
Yes	53 (51.0%)	11 (29.7%)	42 (62.7%)	
Adjuvant hormone therapy				0.861
No	16 (15.4%)	6 (16.2%)	10 (14.9%)	
Yes	88 (84.6%)	31 (83.8%)	57 (85.1%)	

[*] One case tumor size missing imputed as 30 mm. [‡] One case no surgery, high dose radiotherapy, assimilated to lumpectomy. [§] Two cases in each tumor size subgroup had no pathology nodal examination = 0 nodes examined.

Table 2. PET area of hypermetabolism (positivity).

PET area of hypermetabolism	All N = 104	Tumor ≤ 20 mm N = 37	Tumor > 20 mm N = 67 (*)	P-value
PET-Breast positive				< 0.001
Yes	87 (83.7%)	25 (67.6%)	62 (92.5%)	
No	17 (16.3%)	12 (32.4%)	5 (7.5%)	
PET-Axillary positive				0.006
Yes	41 (39.4%)	8 (21.6%)	33 (49.3%)	
No	63 (60.6%)	29 (78.4%)	34 (50.7%)	
PET-Sternal positive				0.906
Yes	6 (5.8%)	2 (5.4%)	4 (6.0%)	
No	98 (94.2%)	35 (94.6%)	63 (94.0%)	
PET-Axillary|Sternal positive				0.019
Yes	44 (42.3%)	10 (27.0%)	34 (50.7%)	
No	60 (57.7%)	27 (73.0%)	33 (49.3%)	

(*) One case tumor size missing imputed as 30 mm.

Table 3. Univariate Cox analysis of overall survival, normalized (nHR) and untransformed (HR1) hazard ratios.

Characteristic	Coding	nHR	P-nHR	HR1	P-HR1
Age (years)	Continuous	2.31	0.010	1.05	0.005
Sex male	Binary	4.10	0.046	8.28	0.046
Upper Outer Quadrant	Binary	0.87	0.718	0.87	0.718
Left laterality[2]	Binary	1.56	0.245	1.56	0.245
Pathological stage[1]	Ordinal 5 levels	3.64	0.001	2.79	0.000
Tumor size (mm)	Continuous	1.64	0.130	1.02	0.070
Number positive nodes (N)	Continuous	2.98	0.001	1.09	0.002
Lymph node ratio (proportion)	Continuous	4.46	0.000	14.8	0.000
Node ratio dichotomized	Binary	3.09	0.002	3.17	0.002
Log odds positive nodes	Continuous	3.47	0.001	1.69	0.001
Estrogen receptor negative	Binary	1.32	0.517	1.35	0.517
Progesterone receptor negative	Binary	3.00	0.003	3.05	0.003
Neu ≥ 2	Binary	1.38	0.404	1.38	0.404
Grade > 2	Binary	1.45	0.329	1.47	0.329
Lymphovascular invasion	Binary	2.45	0.028	2.44	0.028
Ductal histology	Binary	0.87	0.744	0.86	0.744
Primary systemic therapy	Binary	2.02	0.066	2.17	0.066
Mastectomy	Binary	0.99	0.988	0.99	0.988
Adjuvant radiotherapy	Binary	0.88	0.795	0.85	0.795
Adjuvant chemotherapy	Binary	0.91	0.803	0.91	0.803
Adjuvant hormone therapy	Binary	0.60	0.204	0.56	0.204
PET positive Breast	Binary	0.83	0.679	0.82	0.679
PET positive Axillary	Binary	2.26	0.032	2.26	0.032
PET positive Sternal	Binary	2.94	0.010	4.08	0.010
PET Axillary and/or Sternal	Binary	2.77	0.009	2.76	0.009

[1]Stage coded continuous, IIA/B coded 2/2.5. [2]Includes bilateral. Hazard ratio >1 indicates increased risk of death, <1 decreased risk.

Table 4. Multivariate Cox regression on rankit variables.

Starting model with 22 variables, rankit transformed. *Model A*: variables retained after stepwise elimination of weaker ones from the Starting model. *Model B*: same stepwise regression, except lymph node pathology variables excluded from starting (grey shaded, *Omitted*). Normalized hazard ratio (nHR) >1, increased risk of death from any cause; <1, reduced risk. Reliability: percentage of 1000 bootstraps iterations significant at P<0.017 (=0.05 significance by Bonferroni correction), 100% best, 0% worst. [1]Stage coded continuous. [2]Includes bilateral. "—", variable not informative by Akaike information criterion, rejected by stepwise regression.

Characteristic	Starting model		Model A			Model B		
	nHR	P-value	nHR	P-value	Reliability	nHR	P-value	Reliability
Age (years)	2.02	0.168	1.89	0.089	60%	2.91	0.003	78%
Upper Outer Quadrant	1.04	0.938	—	—	—	—	—	—
Left laterality[2]	2.82	0.099	—	—	—	1.85	0.126	38%
• Pathological stage[1]	8.92	0.005	—	—	—		*Omitted*	
Tumor size (mm)	1.11	0.842	—	—	—	—	—	—
• Number positive nodes (N)	0.09	0.040	—	—	—		*Omitted*	
• Lymph node ratio (proportion)	7.39	0.063	5.22	0.000	95%		*Omitted*	
• Node ratio dichotomized	0.46	0.392	—	—	—		*Omitted*	
• Log odds positive nodes	1.86	0.510	—	—	—		*Omitted*	
Estrogen receptor negative	0.28	0.262	—	—	—	—	—	—
Progesterone receptor negative	4.72	0.043	—	—	—	3.05	0.015	72%
Neu ≥ 2	1.18	0.760	—	—	—	—	—	—
Grade > 2	0.69	0.545	—	—	—	—	—	—
Lymphovascular invasion	0.91	0.891	—	—	—	—	—	—
Ductal histology	1.75	0.325	—	—	—	—	—	—
Primary systemic therapy	0.86	0.785	2.00	0.093	45%	—	—	—
Mastectomy	0.57	0.489	—	—	—	—	—	—
Adjuvant radiotherapy	0.31	0.082	—	—	—	—	—	—
Adjuvant chemotherapy	0.68	0.590	0.50	0.143	48%	—	—	—
Adjuvant hormone therapy	0.24	0.099	0.28	0.005	71%	—	—	—
PET positive Breast	0.34	0.157	—	—	—	0.47	0.116	47%
PET Axillary and/or Sternal	2.79	0.113	—	—	—	2.44	0.062	52%

Figures.

Figure 1. Overall survival according to PET status.

The prognostic effect of PET positivity (red) vs. negativity (blue) differs according to the region where positivity is detected: no effect in the Breast, significantly decreased survival in Axillary or Sternal regions. Combining Axillary and Sternal regions provides more robust prognostic separation as shown by the smaller overlap of the 95% confidence dashed bands.

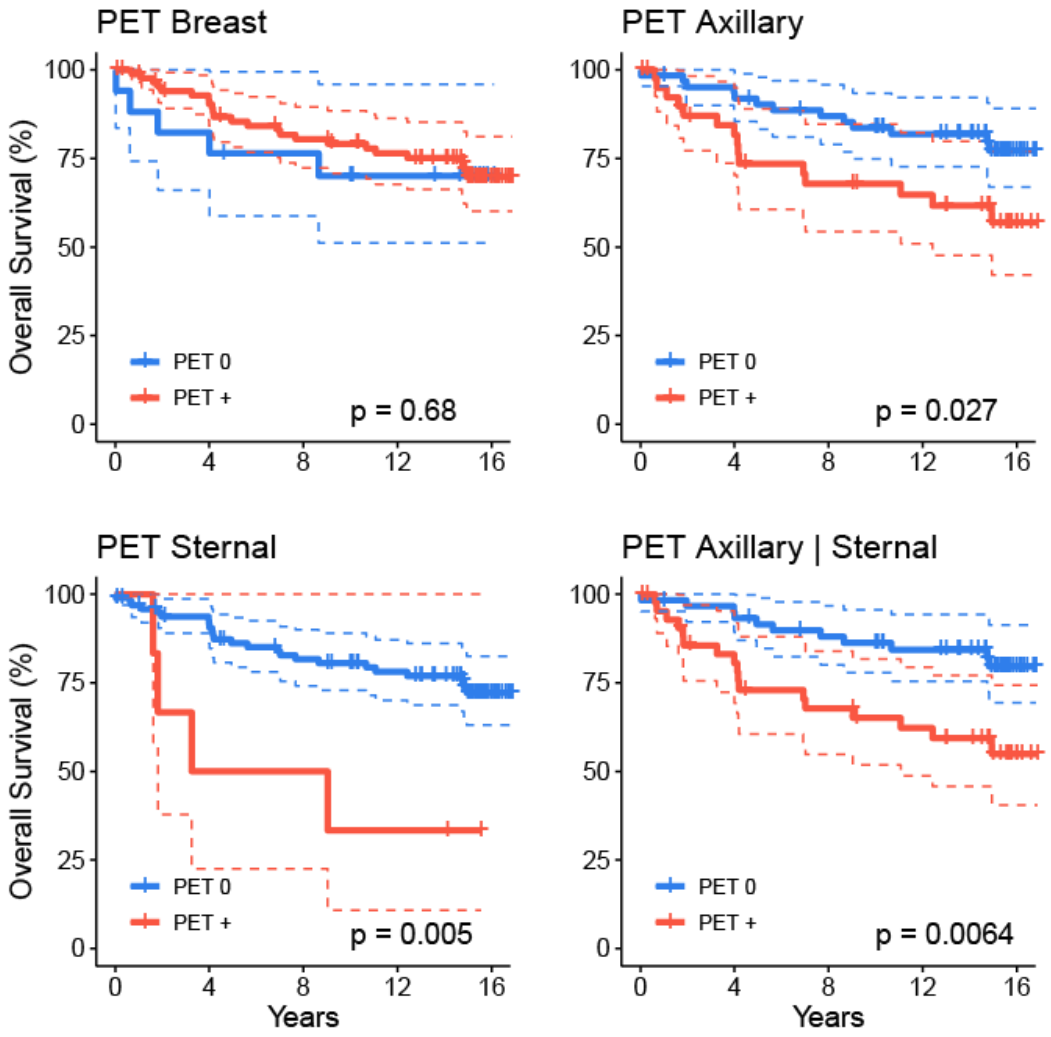

Figure 2. Overlayed survival according to risk group defined by Lymph node ratio (LNR) or by PET Axillary|Sternal status.

P-values refer to pairwise comparisons, LNR ≤ 0.2 vs. PET negative (PET 0), and LNR > 0.2 vs. PET positive (PET +).

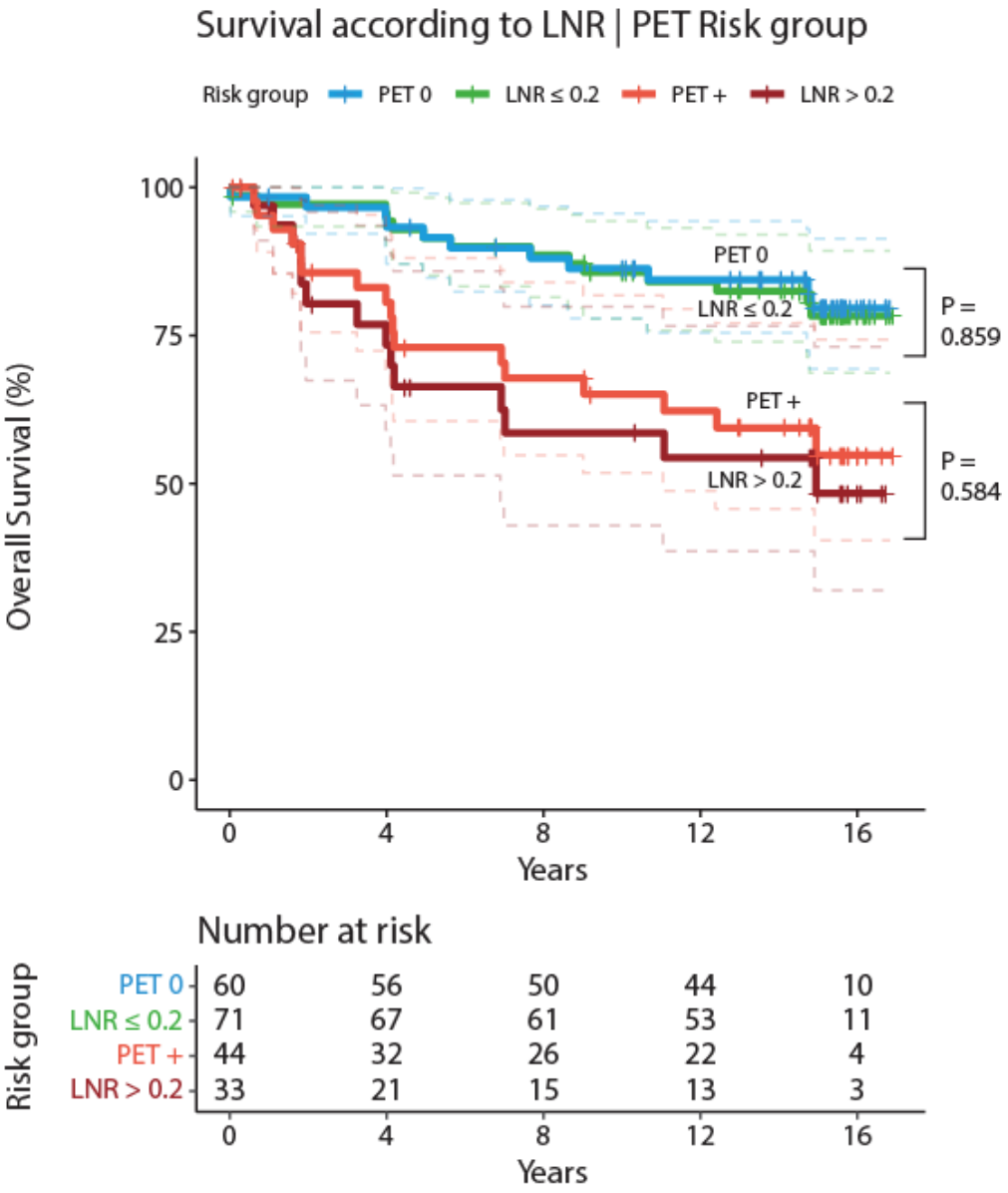

Figure 3. *D* measure of prognostic separation, computed by the absolute of the Log normalized Hazard Ratio.

[1] Stage coded continuous; IIA/B coded 2/2.5. [2] Includes bilateral. • PET variables. Horizontal bar, 95% confidence interval. Vertical bar at *D* = 0, no prognostic separation.

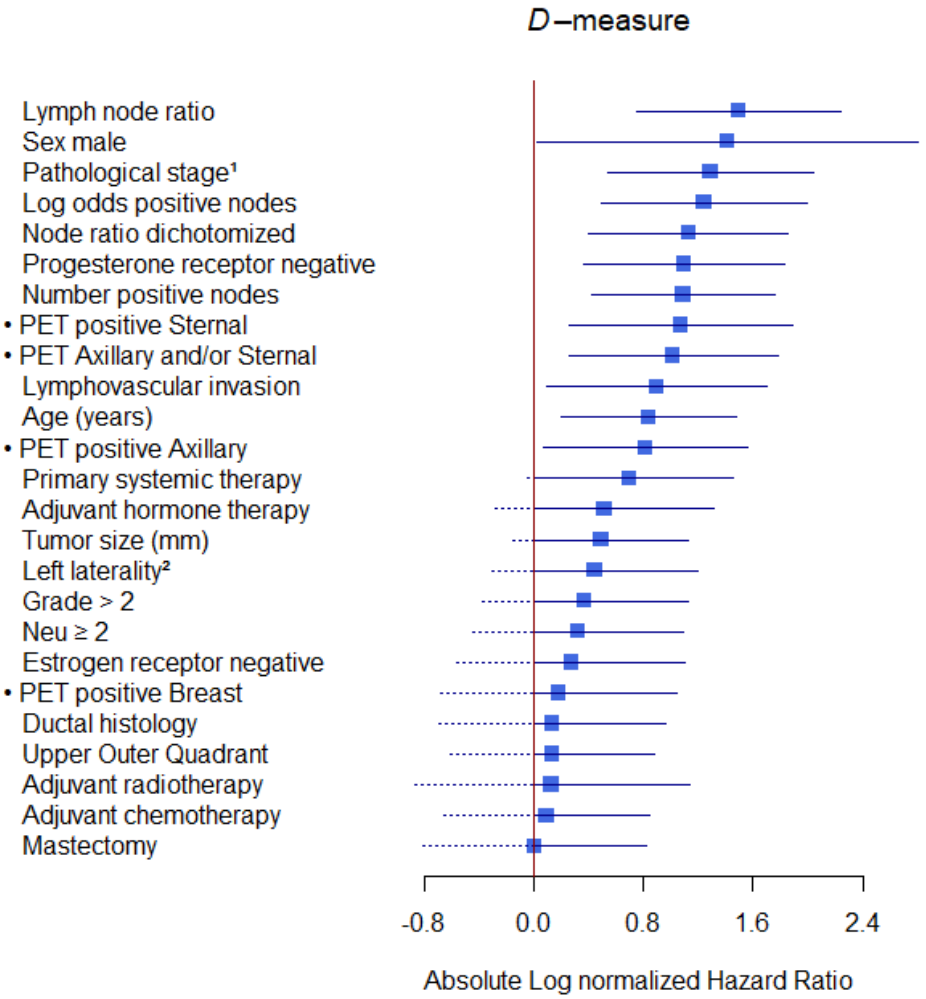

Supplementary Materials

Supplementary Material, Appendix A. R function rnktt.

Description:

Read vector, x
Work on a copy, wx
Get the order, ox
Order the working copy, rx
Compute the rankits, scale them on the fly
If duplicates, get the corresponding mean rankits
Order the rankits according to the original vector
Return the rankits corresponding to the original vector.

Remark: the function ignores missing values, returns missing as-is.

```
#########
#
# rnktt
#
#########
# Description:
# transforms vector x to rankits scaled by sqrt(8/pi)
# Usage:
# rnktt(x)
# Arguments:
# x numeric vector
# Details
# requires function normOrder
# Value:
# returns vector of expected standard Normal order statistics, i.e. rankits
# divided by sqrt(8/pi)
# Author(s)
# Vincent Vinh-Hung, 15 Nov 2020
# References
# Markus S Schröder, Aedín C Culhane, John Quackenbush, Benjamin Haibe-
Kains.
# survcomp, Bioinformatics. 2011 Nov 15; 27(22): 3206–8.
# Patick Royston, Willi Sauerbrei.
# A new measure of prognostic separation in survival data,
# Stat Med. 2004 Mar 15;23(5):723-48
# Bob Wheeler.
# Package 'SuppDists', CRAN. January 18, 2020
#########
```

```
rnktt <- function(x) {
 kap <- sqrt(8/pi)
 wx <- x[!is.na(x)]
 ox <- order(wx)
 rx <- wx[ox]
 rk <- SuppDists::normOrder(N=length(wx)) / kap
 u <- unique(wx[duplicated(wx)])
 for (v in u) { rk[rx==v] <- mean(rk[rx==v]) }
 rr <- x
 rr[!is.na(rr)] <- rk[order(ox)]
 rr
}

#########
```

Supplementary Table ST1. Outcomes.

Outcome	All N = 104	Tumor ≤ 20 mm N = 37	Tumor > 20 mm N = 67 (*)	P-value
Local-regional recurrence				0.652
Yes	4 (3.8%)	1 (2.7%)	3 (4.5%)	
No	100 (96.2%)	36 (97.3%)	64 (95.5%)	
New primary tumor				0.759
Yes	10 (9.6%)	4 (10.8%)	6 (9.0%)	
No	94 (90.4%)	33 (89.2%)	61 (91.0%)	
Metastases				0.645
Yes	31 (29.8%)	10 (27.0%)	21 (31.3%)	
No	73 (70.2%)	27 (73.0%)	46 (68.7%)	
Death				0.365
Yes	28 (26.9%)	8 (21.6%)	20 (29.9%)	
No	76 (73.1%)	29 (78.4%)	47 (70.1%)	

(*) One case tumor size missing imputed as 30 mm.

Supplementary Figure SF1. Map of missing-data patterns.

Bottom row = number of records missing for the corresponding variable shown on the top row; example, *neurecod* missing 1 record. Left column = number of records having the same missing pattern. Right column = number of missing variables; example 35 records (left column) had 1 variable (right column) missing shown in red, *ki67*. HER2 Fish ratio, HER2 Fish, HER2 Cen17 and Ki67 were missing in 51, 53, 53 and 101 cases; these variables were not considered for analyses. Non-missing variables are not shown.

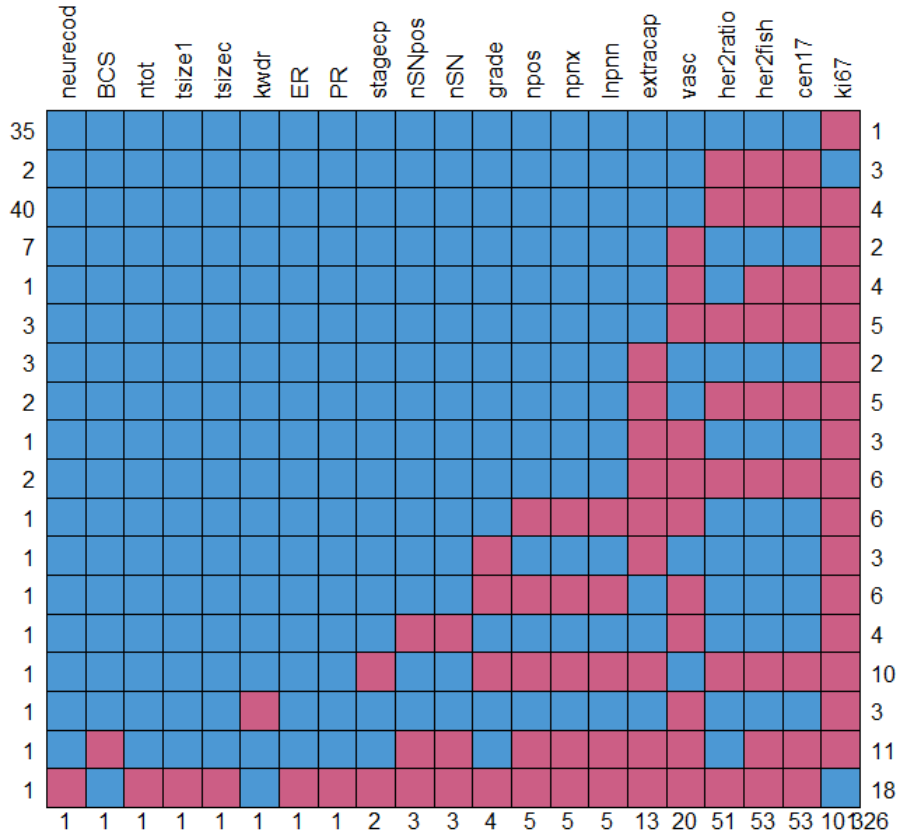

Supplementary Figure SF2. Survival according to PET status or Lymph node ratio (LNR) and according to tumor size.

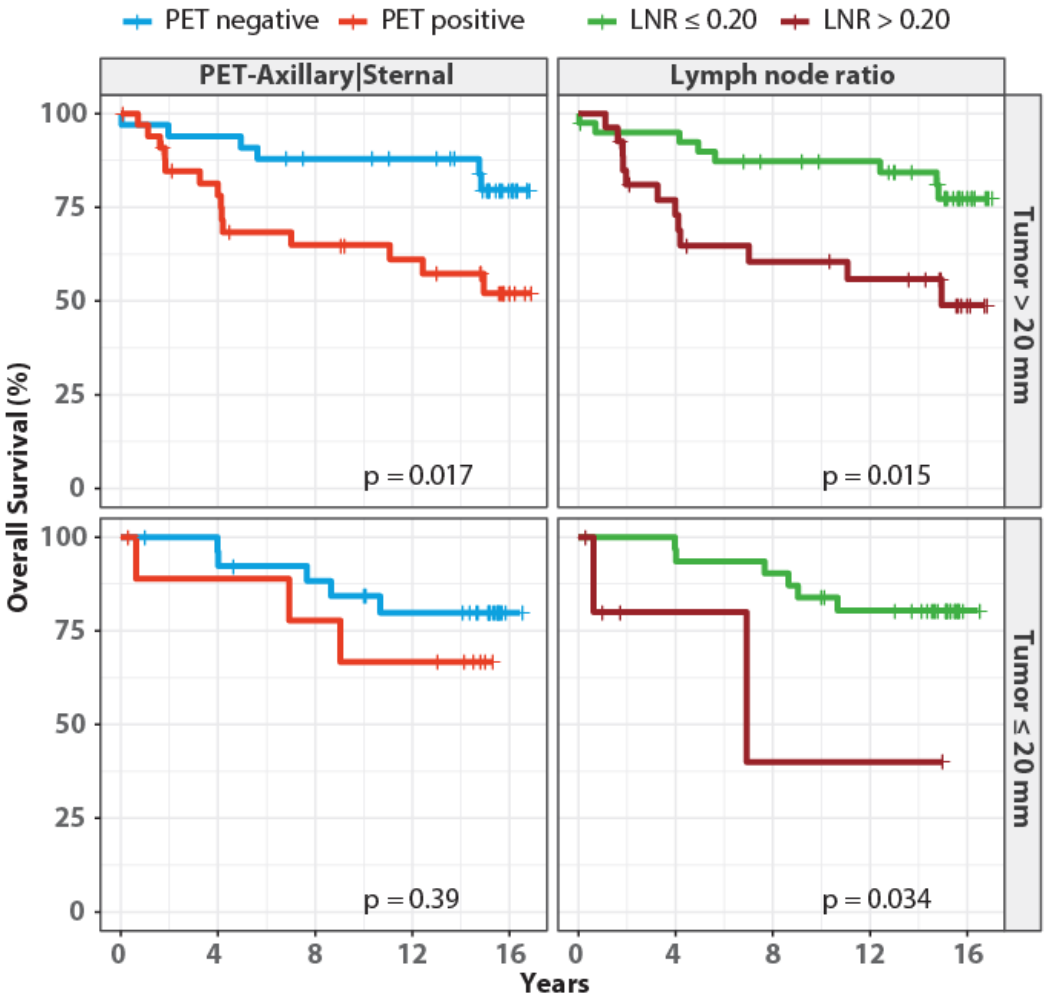

Supplementary Figure SF3. PET-Axillary|Sternal positivity as a function of the Lymph node ratio.

White curve: logistic regression. Grey band: 95% confidence. Histograms: red, PET positive; blue, PET negative.